Structure of shock compressed model basaltic glass: Insights from O K-edge X-ray Raman scattering and high-resolution ^{27}Al NMR spectroscopy

Sung Keun Lee,[1] Sun Young Park,[1] Hyo-Im Kim,[1] Oliver Tschauner,[2] Paul Asimow,[3] Ligang Bai,[2] Yuming Xiao,[4] and Paul Chow[4]

Received 9 January 2012; revised 3 February 2012; accepted 7 February 2012; published 3 March 2012.

[1] The detailed atomic structures of shock compressed basaltic glasses are not well understood. Here, we explore the structures of shock compressed silicate glass with a diopside–anorthite eutectic composition ($Di_{64}An_{36}$), a common Fe-free model basaltic composition, using oxygen K-edge X-ray Raman scattering and high- resolution ^{27}Al solid-state NMR spectroscopy and report previously unknown details of shock-induced changes in the atomic configurations. A topologically driven densification of the $Di_{64}An_{36}$ glass is indicated by the increase in oxygen K-edge energy for the glass upon shock compression. The first experimental evidence of the increase in the fraction of highly coordinated Al in shock compressed glass is found in the ^{27}Al NMR spectra. This unambiguous evidence of shock-induced changes in Al coordination environments provides atomistic insights into shock compression in basaltic glasses and allows us to microscopically constrain the magnitude of impact events or relevant processes involving natural basalts on Earth and planetary surfaces. **Citation:** Lee, S. K., S. Y. Park, H.-I. Kim, O. Tschauner, P. Asimow, L. Bai, Y. Xiao, and P. Chow (2012), Structure of shock compressed model basaltic glass: Insights from O K-edge X-ray Raman scattering and high-resolution ^{27}Al NMR spectroscopy, *Geophys. Res. Lett.*, *39*, L05306, doi:10.1029/2012GL050861.

1. Introduction

[2] The structures of shock compressed silicate glasses and melts, including basalts, are essential to understand the changes in the corresponding melt properties under dynamic compression and to provide atomistic insights into impact-induced events in Earth's crust and planetary surfaces [*Akins et al.*, 2004; *Okuno et al.*, 1999; *Reynard et al.*, 1999; *Shimoda et al.*, 2004; *Tschauner et al.*, 2009]. Knowing the structures of shock compressed basaltic glasses also provide an atomistic understanding of the geophysical processes involving basaltic magmas in the Earth's interior [*Asimow and Ahrens*, 2010; *Rigden et al.*, 1988]. The Ca-Mg aluminosilicate melt of diopside–anorthite eutectic composition ($Di_{64}An_{36}$) can serve as a model system for basaltic melts [*Ai and Lange*, 2008; *Milholland and Presnall*, 1998]. Despite the importance, shock-induced structural changes in basaltic glasses have not been well understood. Part of the difficulty arises from the prominent disorder inherent in multicomponent silicate glasses that makes it difficult to resolve their atomic structures. Nevertheless, previous vibrational spectroscopic and X-ray scattering studies of shock compressed silica and diverse silicate glasses reported a reduction of the inter-tetrahedral angle with increasing shock pressure up to ~25 GPa and an increase in the fraction of smaller-membered rings [*Okuno et al.*, 1999; *Reynard et al.*, 1999; *Shimada et al.*, 2002, 2004]. Recent ^{11}B NMR spectra for Al-bearing Na-borosilicate glass showed that the fraction of non-ring species increase with peak shock pressure [*Manghnani et al.*, 2011]. All these previously reported structural changes result from topological rearrangements without changes in the coordination number of framework cations (e.g., Si and Al). This is in contrast to pressure-induced changes in short-range structure in silicate melts under static compression, where increases in the coordination number of Si and Al with pressure occur [e.g., *Allwardt et al.*, 2007; *Kelsey et al.*, 2009; *Lee et al.*, 2003; *Xue et al.*, 1991; *Yarger et al.*, 1995]. This difference was partly attributed to high residual temperature, which may allow post-shock annealing of the network structure into low-density phases [*Shimoda et al.*, 2004], but it could be partly due to a lack of suitable experimental probes of local structure of multicomponent oxide glasses.

[3] The nature of permanent densification in model basaltic glasses under dynamic compression can be probed using recently developed element-specific structural probes, such as X-ray Raman scattering (XRS) and 2D solid-state NMR spectroscopy. XRS has been effective in probing electronic structures around low-Z elements such as O, and C in Earth materials at high pressure [*Lee et al.*, 2005a, 2005b; *Mao et al.*, 2003; *Meng et al.*, 2008]. In particular, oxygen K-edge XRS for SiO_2 and $MgSiO_3$ polymorphs show distinct K-edge features stemming from their local atomic configurations and topology around oxygen [*Fukui et al.*, 2009; *Lee et al.*, 2008; *Lin et al.*, 2007]. An increase in the fraction of the O K-edge feature at 544–545 eV in $MgSiO_3$ glass was suggested to be due to oxygen coordination transformation [*Lee et al.*, 2008]. We apply O K-edge XRS to explore the structure of multicomponent glasses, revealing the shock-induced transitions in atomic environments around oxygen in unshocked and shocked $Di_{64}An_{36}$ glasses.

[1]School of Earth and Environmental Sciences, Seoul National University, Seoul, South Korea.
[2]High Pressure Science and Engineering Center, Department of Geology/Physics and Astronomy, University of Nevada, Las Vegas, Las Vegas, Nevada, USA.
[3]Division of Geological and Planetary Sciences, California Institute of Technology, Pasadena, California, USA.
[4]HPCAT, Geophysical Laboratory, Carnegie Institution of Washington, Argonne, Illinois, USA.

0094-8276/12/2012GL050861

[4] Progress in 2D triple-quantum magic-angle spinning (3QMAS) NMR has yielded detailed Al coordination environments and measurements of topological disorder due to distortion of glass networks in 'multicomponent' aluminosilicate glasses [*Lee et al.*, 2005a, 2005b; *Neuville et al.*, 2008; *Xue and Kanzaki*, 2008]. Studies of the model basaltic glass at 1 atm revealed the presence of a low percentage of $^{[5]}$Al and defined the degree of network polymerization [*Xue and Kanzaki*, 2008]. With increasing static pressure, ^{27}Al 3QMAS NMR studies have shown an increasing fraction of highly coordinated $^{[5,6]}$Al in aluminosilicate glasses [*Lee*, 2011]. Application of the high-resolution NMR technique to shock compressed glass therefore reveal the effect of shock compression on coordination number and network polymerization in basaltic glasses. In this study, we explore the effect of shock compression on the structure of model basaltic glass to reveal the nature of permanent densification in glasses under dynamic compression and report the first O K-edge XRS and 2D ^{27}Al NMR spectra for shock compressed $Di_{64}An_{36}$ recovered from a peak pressure of 20 GPa. We discuss the relationship between shock compression and the Al coordination number in shocked glass, which provide atomistic insights into terrestrial and planetary impact events.

2. Experimental Methods

2.1. Glass Synthesis and Shock Wave Experiment

[5] The starting glass was prepared as documented by *Asimow and Ahrens* [2010] by powdering, mixing, and melting initial glasses with diopside and anorthite composition synthesized by Dow Corning Corporation. Electron probe analysis is given by *Asimow and Ahrens* [2010]; the composition is close to the nominal $Di_{64}An_{36}$ eutectic, with minor Na_2O (0.067 $\pm$ 0.021 wt.%) and barely resolved FeO (0.018 $\pm$ 0.016 wt.%). A disk 0.5 mm thick of 5 mm diameter was loaded into a cavity in a stainless steel 304 (SS304) chamber with 5.5 mm of steel between impact surface and sample, acting as driver. A 0.5 mm thick SS304 flyer attached to a Lexan sabot was launched into the driver at 1.67 km/s by a 20 mm bore single-stage propellant gun. The full time history of wave interactions and the thermodynamic path of the sample are imposed by geometry and material properties. The first shock brought the sample to pressure ~15 GPa and average temperature ~650 K and increased its density by ~25%. The first reshock, reflected off the SS304 rear chamber surface, further increased pressure to ~20 GPa, average temperature to ~900 K, and density by a further 5%. The rarefaction wave originating at the rear flyer surface released the sample back to 1 bar pressure and an average post-shock temperature of ~700 K, after which it conductively cooled to room temperature. In local regions, focusing of the shock front by topography at the driver-sample interface caused increases in temperature sufficient to melt the sample (1 bar liquidus temperature is 1547 K). The state of the recovered product is thus the result of a temporally and spatially inhomogeneous loading history. However, the melted region was clearly distinguishable as a several μm-size mixture of silicate and iron-rich metal. Its volume is negligible, yielding little contribution to both XRS and NMR spectra. Additionally, we removed that part of the glass that contained visible metal droplets by hand-picking under binocular microscope. The resulting glass particles were thus all from the portion of the shocked sample which had not been melted. Recovered features also suggest permanent densification in bulk recovered sample away from these hotspots. The structure of shock compressed glass studied here represents irreversibly densified glass from P-T conditions along the adiabatic shock release path but below its glass transition temperature.

2.2. X-Ray Raman Spectroscopy

[6] The X-ray Raman spectra for the unshocked and shocked $Di_{64}An_{36}$ glass were collected at HPCAT sector 16ID-D of the Advanced Photon Source. X-ray Raman spectra were collected for the samples (~200 μm) attached to 100-μm glass fibers mounted directly on the goniometer. The spectra were collected by scanning the energy of the incident beam relative to the analyzer with a fixed elastic energy (E_0) of ~9.886 keV at a scattering angle of 20°. A linear array of 17 spherical Si(555) analyzers operating in a backscattering geometry was used. The X-ray beam size was approximately 50 μm(H) * 30 μm(V). The sample was located in the beam such that the glass fiber generates no contributions to the spectrum. X-ray Raman spectra were collected with 0.5 eV steps. Raw X-ray Raman spectra were background-subtracted.

2.3. NMR Spectroscopy

[7] The ^{27}Al NMR spectra of the $Di_{64}An_{36}$ glass were collected using a Varian solid-state NMR 400 system at 104.23 MHz (9.4 T) with a 3.2 mm Varian double- resonance probe (Seoul National University, Korea). For MAS spectra, a relaxation delay of 1 s with an *rf* pulse length of 0.3 μs were used with spinning speed of 17 kHz. Because there was also signal due to the background from the empty rotors and small sample volume (~3–4 mg) of the shock compressed sample, the final spectrum for shock compressed glass was obtained after subtraction of the background signals. Enhancement of signal intensity of the shock compressed sample was achieved by locating the available sample at the center of NMR rotor, which also allows us to collect 3QMAS NMR spectrum despite small sample volume. For 3QMAS NMR spectra, a fast amplitude modulation (FAM)-based shifted-echo pulse sequence (3.0 μs – t_2 delay – $[0.6\ \mu s]_{FAM}$ - echo delay-15 μs) with a relaxation delay of 1 s was used. The ^{27}Al NMR spectra were referenced to an external 0.3 M $AlCl_3$ solution.

3. Results and Discussion

[8] Figure 1 shows the O K-edge XRS spectra for unshocked (black) and shocked $Di_{64}An_{36}$ glass (red). A dominant peak at 538–540 eV is shown for the spectrum for both unshocked and shocked glass. The feature is similar to those observed for the O K-edge XRS spectra of SiO_2 and $MgSiO_3$ glasses at 1 atm and is due to an excitation of an electron from the oxygen 1*s*-state into unoccupied oxygen 2*p*-states hybridized with the silicon 3*s*- and 3*p*-states of $^{[4]}$Si [*Lee et al.*, 2008; *Lin et al.*, 2007]. After shock compression, a slight edge energy shift of approximately 1 eV is observed. Taking into consideration the uncertainty due to overall low signal/background ratio of the spectrum and insufficient signal averaging, the observed shift in the K-edge feature

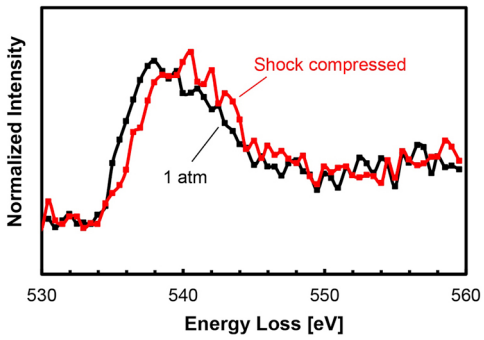

Figure 1. Oxygen K-edge XRS spectra for glass with a diopside–anorthite eutectic composition ($Di_{64}An_{36}$) quenched from melts at 1 atm (black) and recovered after shock compression (red). The spectra were plotted as energy loss (incident energy − elastic energy) *vs.* normalized scattered intensity.

may not be regarded as evidence for noticeable structural transitions after shock compression. Nevertheless, O K-edge features move slightly to higher energy with structural densification in Mg-silicate polymorphs from enstatite, ilmenite, to perovskite due to an increase in the energy of unoccupied oxygen 2*p*-state with pressure [*Lee et al.*, 2008]. The current result thus suggests a densification of the $Di_{64}An_{36}$ glass upon shock compression. The shock-induced energy shift in the O K-edge is due to topological changes (e.g., a reduction in the bond angle, typical shift of ~1–2 eV) in the glass structure, as indicated by a lack of a feature at ~543–545 eV (that may stem from the formation of triply coordinated oxygen) [*Lee et al.*, 2008]. A similar edge-energy shift in permanently densified $MgSiO_3$ glass was also observed [*Lee et al.*, 2008].

[9] Figure 2 shows ^{27}Al MAS NMR spectra for the $Di_{64}An_{36}$ glass quenched from the melt at 1 atm and recovered after shock wave compression. The broad features at ~60 ppm indicate that $^{[4]}$Al is dominant at 1 atm, and the longer tail on the lower frequency shoulder indicate the topological disorder in this glass, which is typical for aluminosilicate glasses. After shock compression, the center of gravity of the peak apparently moves to more negative chemical shift and the peak width increases, demonstrating shock-induced structural changes in the glass. The observed change may be due to shock-induced increase in topological disorder around Al that increases the ^{27}Al quadrupolar coupling constant ($C_q = P_q/(1 + \eta^2/3)^{1/2}$, where P_q and η are the quadrupolar coupling product and the asymmetry parameter, respectively), which results in the increase in peak width in the MAS NMR spectrum. It may also be explained by the formation of highly coordinated Al (i.e., $^{[5,6]}$Al); the $^{[5,6]}$Al peak positions are ~30 and 0 ppm, respectively but theses peaks largely overlap with lower frequency tail of $^{[4]}$Al peak in the ^{27}Al MAS NMR. The 3QMAS NMR measurement can help to resolve this ambiguity.

[10] Figure 3 shows ^{27}Al 3QMAS NMR spectra for the $Di_{64}An_{36}$ glass quenched from melt at 1 atm and retrieved after shock compression; the $^{[4,5,6]}$Al peaks are well resolved. The spectrum of the glass at 1 atm predominantly shows $^{[4]}$Al and a minor but non-negligible fraction of $^{[5]}$Al, consistent with the previous studies [*Xue and Kanzaki*, 2008]. After shock compression, the fraction of $^{[5]}$Al in the glass apparently increases, providing the first evidence for the shock-induced Al coordination transformation in the glasses. Feature due to $^{[6]}$Al is visible, which partly stems from the rotor background (see below). The ^{27}Al C_q for $^{[4]}$Al obtained from the center of gravity of the $^{[4]}$Al peak (with η of 0.5) in the 2D spectrum slightly increases from ~6.2 MHz (unshocked) to ~6.4 MHz (shocked), implying that network distortion around Al (and thus the topological disorder) is larger for the shocked glass [*Park and Lee*, 2012]. Figure 4 shows the total isotropic projections of the unshocked and shocked ^{27}Al 3QMAS NMR spectra for the $Di_{64}An_{36}$ glass. The results here are qualitative as the estimation of the fraction of a small amount of $^{[5]}$Al in 2D NMR is not trivial. It is, however, apparent from the spectra that the fraction of $^{[4]}$Al decreases upon shock compression, while the fraction of $^{[5]}$Al increase noticeably. Rotor background signal contributes to total $^{[6]}$Al peak intensity (blue spectrum). In addition to increase in the $^{[5]}$Al fraction, the spectrum shows that the peak maximum of $^{[4]}$Al in the projection shifts to a lower frequency and the peak width for $^{[4]}$Al in the isotropic projection apparently increases after shock compression. This is partly because the fractions of $Q^4(n\text{Si})$ with smaller n (Al^{3+} is surrounded by n $^{[4]}$Si as the next nearest neighbors) increase upon shock compression, suggesting an increase in the Al–O–Al fraction (and configurational disorder) upon shock compression.

[11] The current experimental results highlight the contribution of shock-induced topological changes in the model basaltic glass structure to overall permanent densification upon shock compression, consistent with previous studies [*Okuno et al.*, 1999; *Reynard et al.*, 1999; *Shimoda et al.*, 2004]. Additionally, the clear evidence of Al coordination increase found here differs from previous studies, which have not documented changes in short-range structure. Previous studies differed from this one in the choice of analytical probes, in experimental shock recovery techniques, and in the studied glass compositions. The current methods offer new and precise constraints on shock-induced structural changes in $Di_{64}An_{36}$ glass by probing the oxygen and aluminum environments. We also consider the details of the recovery methods and the resulting rates and pressure-temperature paths of shock compression, release, and post-shock relaxation. For example, observed structural differences between shocked and unshocked glasses were

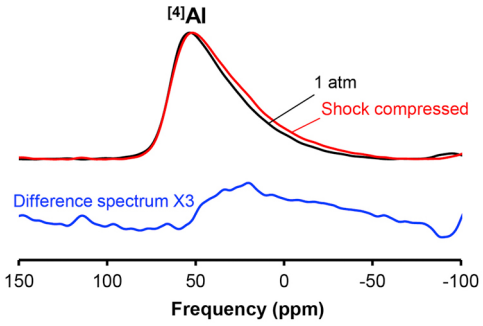

Figure 2. ^{27}Al MAS NMR spectra (collected at 9.4 T) of $Di_{64}An_{36}$ glass quenched from melt at 1 atm (black) and recovered after shock compression (red). The blue line shows a difference spectrum.

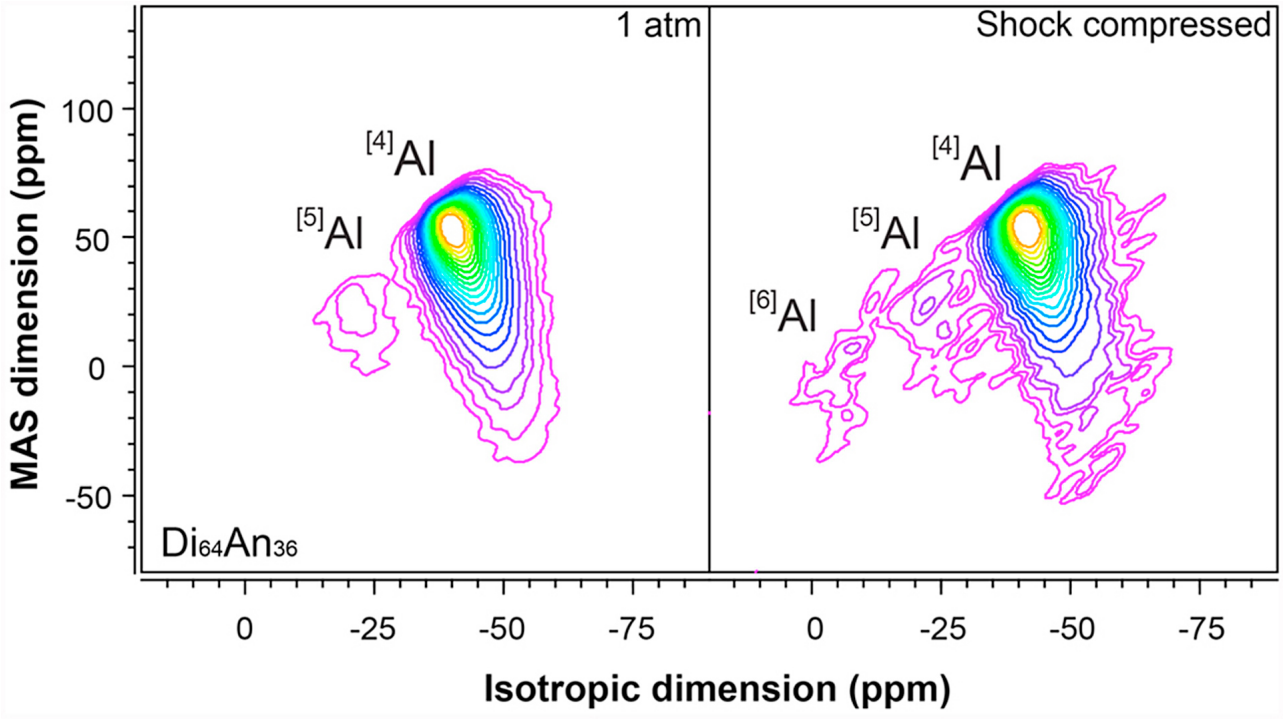

Figure 3. ^{27}Al 3QMAS NMR spectra (collected at 9.4 T) of $Di_{64}An_{36}$ glass quenched from melt (left) at 1 atm and (right) recovered after shock compression. Contour lines are drawn at 5% intervals from relative intensities of 12% to 87%, with added lines at 2, 3.5, 6, and 8%.

suggested to result partly from variations in the glass transition temperature during relaxation after shock compression [*Manghnani et al.*, 2011]. In the current study, the complete pressure-temperature path of compression, release, and cooling took place below the glass transition. The observed structural changes are, thus, due to shock-induced permanent densification in the glasses. Composition is an important difference between this and previous studies, as well. Previous NMR results on glasses quenched from static high pressure show strong links between structural transitions in glasses and composition: the $^{[5,6]}$Al fraction in melts at high pressure increases with increasing cation field strength (i.e., charge/ionic radius) of non-network forming cations [*Allwardt et al.*, 2007]. The formation of shock-induced changes in the Al coordination environment in this study of a Ca-Mg aluminosilicate glass thus results from the presence of Mg^{2+} as non-network forming cations, which facilitates the formation of $^{[5,6]}$Al at high pressure. Note that probing atomic structures of glasses with more than ~5 wt. % of paramagnetic element (e.g., Fe) using NMR has been met with limited success. The effect of iron content on the structure of shock compressed glass therefore remains to be explored. Finally, the structure of the dynamically compressed glass is distinct from that of glass quenched from corresponding liquid at high pressure. On-going analysis of basaltic glass quenched from melts at high pressure will unveil the structure of supercooled basaltic melts.

[12] The first observation of minor (but detectable) shock-induced formation of $^{[5]}$Al in the model basaltic glass provides an atomistic insight into shock compression and impact events involving basalts, which are wide-spread in the inner solar system. While it is speculative, we predict that any relevant impact events on basalts, whether on Earth, Mars, the Moon, or asteroid surfaces, may lead to the formation of $^{[5]}$Al in glasses with compositions similar to that studied here. In addition to popular shock indices based on the stability or (in a few cases, thresholds for shock recovery) of dense crystalline minerals or the formation of mineral assemblages relevant to impact events [*Collerson et al.*, 2010; *Gupta et al.*, 2001; *Miyahara et al.*, 2011; *Ohtani*, 2009; *Tschauner et al.*, 2009], the estimation of Al site fractions in impact glasses in Earth and other planetary surfaces, lunar glasses, and shocked meteorites may yield shock pressure estimates. Additionally, the irreversible

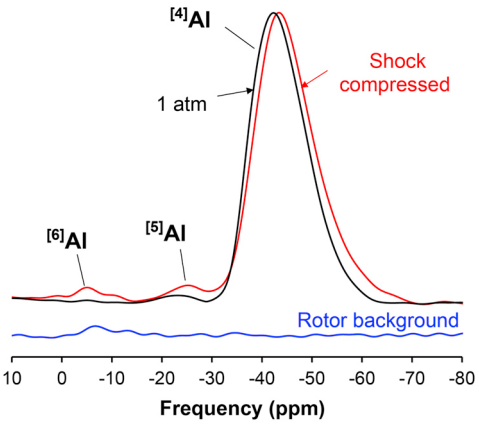

Figure 4. Total isotropic projection of ^{27}Al 3QMAS NMR for $Di_{64}An_{36}$ glass quenched from melt at 1 atm (black) and recovered after shock compression (red). Isotropic projection of the spectrum for rotor background with $^{[6]}$Al is also shown (blue).

structural transitions in metastable glasses are inevitably path-dependent, which in turn allows us to uniquely explore the detailed pressure-temperature-time path and relevant rate processes upon asteroid impacts. Future study of the systematics of quantitative Al site fractions in natural impact glasses and in experimentally-derived key multi-component glasses with varying peak pressures, composition, and thermal history therefore lead to new constraints on the magnitude or duration of impact events and related processes, during collisional evolution in the early solar system or on planetary surfaces of all ages.

[13] **Acknowledgments.** This work was supported by the National Research Foundation, Korea to S.K.L. (2007-000-20120) and through subcontract 675P of NNSA DE-FC88-01NV14049 to O.T.. HPCAT was supported by DOE-BES-Materials Science, DOE-NNSA, CDAC, NSF, DOD–TACOM, and the W.M. Keck Foundation. The Caltech shock wave lab is supported by NSF EAR-1119522. We thank two anonymous reviewers for constructive comments.

[14] The Editor thanks two anonymous reviewers for their assistance in evaluating this paper.

References

Ai, Y. H., and R. A. Lange (2008), New acoustic velocity measurements on CaO-MgO-Al_2O_3-SiO_2 liquids: Reevaluation of the volume and compressibility of $CaMgSi_2O_6$-$CaAl_2Si_2O_8$ liquids to 25 GPa, *J. Geophys. Res.*, *113*, B04203, doi:10.1029/2007JB005010.

Akins, J. A., S. N. Luo, P. D. Asimow, and T. J. Ahrens (2004), Shock-induced melting of $MgSiO_3$ perovskite and implications for melts in Earth's lowermost mantle, *Geophys. Res. Lett.*, *31*, L14612, doi:10.1029/2004GL020237.

Allwardt, J. R., J. F. Stebbins, H. Terasaki, L. S. Du, D. J. Frost, A. C. Withers, M. M. Hirschmann, A. Suzuki, and E. Ohtani (2007), Effect of structural transitions on properties of high-pressure silicate melts: Al-27 NMR, glass densities, and melt viscosities, *Am. Mineral.*, *92*(7), 1093–1104, doi:10.2138/am.2007.2530.

Asimow, P. D., and T. J. Ahrens (2010), Shock compression of liquid silicates to 125 GPa: The anorthite-diopside join, *J. Geophys. Res.*, *115*, B10209, doi:10.1029/2009JB007145.

Collerson, K. D., Q. Williams, B. S. Kamber, S. Omori, H. Arai, and E. Ohtani (2010), Majoritic garnet: A new approach to pressure estimation of shock events in meteorites and the encapsulation of sub-lithospheric inclusions in diamond, *Geochim. Cosmochim. Acta*, *74*(20), 5939–5957, doi:10.1016/j.gca.2010.07.005.

Fukui, H., M. Kanzaki, N. Hiraoka, and Y. Q. Cai (2009), X-ray Raman scattering for structural investigation of silica/silicate minerals, *Phys. Chem. Miner.*, *36*(3), 171–181, doi:10.1007/s00269-008-0267-x.

Gupta, S. C., T. J. Ahrens, and W. B. Yang (2001), Shock-induced vaporization of anhydrite and global cooling from the K/T impact, *Earth Planet. Sci. Lett.*, *188*(3–4), 399–412, doi:10.1016/S0012-821X(01)00327-2.

Kelsey, K. E., J. F. Stebbins, J. L. Mosenfelder, and P. D. Asimow (2009), Simultaneous aluminum, silicon, and sodium coordination changes in 6 GPa sodium aluminosilicate glasses, *Am. Mineral.*, *94*(8–9), 1205–1215, doi:10.2138/am.2009.3177.

Lee, S. K. (2011), Simplicity in melt densification in multi-component magmatic reservoirs in Earth's interior revealed by multi-nuclear magnetic resonance, *Proc. Natl. Acad. Sci. U. S. A.*, *108*(17), 6847–6852, doi:10.1073/pnas.1019634108.

Lee, S. K., Y. Fei, G. D. Cody, and B. O. Mysen (2003), Order and disorder of sodium silicate glasses and melts at 10 GPa, *Geophys. Res. Lett.*, *30*(16), 1845, doi:10.1029/2003GL017735.

Lee, S. K., G. D. Cody, and B. O. Mysen (2005a), Structure and the extent of disorder in quaternary (Ca-Mg and Ca-Na) aluminosilicate glasses and melts, *Am. Mineral.*, *90*(8–9), 1393–1401, doi:10.2138/am.2005.1843.

Lee, S. K., P. J. Eng, H. K. Mao, Y. Meng, M. Newville, M. Y. Hu, and J. F. Shu (2005b), Probing of bonding changes in B_2O_3 glasses at high pressure with inelastic x-ray scattering, *Nat. Mater.*, *4*, 851–854, doi:10.1038/nmat1511.

Lee, S. K., et al. (2008), X-ray Raman scattering study of $MgSiO_3$ glass at high pressure: Implication for triclustered $MgSiO_3$ melt in Earth's mantle, *Proc. Natl. Acad. Sci. U. S. A.*, *105*(23), 7925–7929, doi:10.1073/pnas.0802667105.

Lin, J. F., et al. (2007), Electronic bonding transition in compressed SiO_2 glass, *Phys. Rev. B*, *75*(1), 012201, doi:10.1103/PhysRevB.75.012201.

Manghnani, M. H., A. Hushur, T. Sekine, J. Wu, J. F. Stebbins, and Q. Williams (2011), Raman, Brillouin, and nuclear magnetic resonance spectroscopic studies on shocked borosilicate glass, *J. Appl. Phys.*, *109*(11), 113509, doi:10.1063/1.3592346.

Mao, W. L., H. K. Mao, P. J. Eng, T. P. Trainor, M. Newville, C. C. Kao, D. L. Heinz, J. F. Shu, Y. Meng, and R. J. Hemley (2003), Bonding changes in compressed superhard graphite, *Science*, *302*, 425–427, doi:10.1126/science.1089713.

Meng, Y., P. J. Eng, J. S. Tse, D. M. Shaw, M. Y. Hu, J. F. Shu, S. A. Gramsch, C. Kao, R. J. Hemley, and H. K. Mao (2008), Inelastic X-ray scattering of dense solid oxygen: Evidence for intermolecular bonding, *Proc. Natl. Acad. Sci. U. S. A.*, *105*(33), 11,640–11,644, doi:10.1073/pnas.0805601105.

Milholland, C. S., and D. C. Presnall (1998), Liquidus phase relations in the CaO-MgO-$Al2O_3$-SiO_2 system at 3.0 GPa: The aluminous pyroxene thermal divide and high-pressure fractionation of picritic and komatiitic magmas, *J. Petrol.*, *39*(1), 3–27, doi:10.1093/petrology/39.1.3.

Miyahara, M., E. Ohtani, M. Kimura, S. Ozawa, T. Nagase, M. Nishijima, and K. Hiraga (2011), Evidence for multiple dynamic events and subsequent decompression stage recorded in a shock vein, *Earth Planet. Sci. Lett.*, *307*(3–4), 361–368, doi:10.1016/j.epsl.2011.05.010.

Neuville, D. R., L. Cormier, V. Montouillout, P. Florian, F. Millot, J. C. Rifflet, and D. Massiot (2008), Structure of Mg- and Mg/Ca aluminosilicate glasses: ^{27}Al NMR and Raman spectroscopy investigations, *Am. Mineral.*, *93*(11–12), 1721–1731, doi:10.2138/am.2008.2867.

Ohtani, E. (2009), Melting relations and the equation of state of magmas at high pressure: Application to geodynamics, *Chem. Geol.*, *265*(3–4), 279–288, doi:10.1016/j.chemgeo.2009.04.004.

Okuno, M., B. Reynard, Y. Shimada, Y. Syono, and C. Willaime (1999), A Raman spectroscopic study of shock-wave densification of vitreous silica, *Phys. Chem. Miner.*, *26*(4), 304–311, doi:10.1007/s002690050190.

Park, S. Y., and S. K. Lee (2012), Structure and disorder in basaltic glasses and melts: Insights from high-resolution solid-state NMR study of glasses in diopside–Ca-tschermakite join and diopside–anorthite eutectic composition, *Geochim. Cosmochim. Acta*, *80*, 125–142, doi:10.1016/j.gca.2011.12.002.

Reynard, B., M. Okuno, Y. Shimada, Y. Syono, and C. Willaime (1999), A Raman spectroscopic study of shock-wave densification of anorthite ($CaAl_2Si_2O_8$) glass, *Phys. Chem. Miner.*, *26*(6), 432–436, doi:10.1007/s002690050205.

Rigden, S. M., T. J. Ahrens, and E. M. Stolper (1988), Shock compression of molten silicate - results for a model basaltic composition, *J. Geophys. Res.*, *93*(B1), 367–382, doi:10.1029/JB093iB01p00367.

Shimada, Y., M. Okuno, Y. Syono, M. Kikuchi, K. Fukuoka, and N. Ishizawa (2002), An X-ray diffraction study of shock-wave-densified SiO_2 glasses, *Phys. Chem. Miner.*, *29*(4), 233–239, doi:10.1007/s00269-001-0235-1.

Shimoda, K., M. Okuno, Y. Syono, M. Kikuchi, K. Fukuoka, M. Koyano, and S. Katayama (2004), Structural evolutions of an obsidian and its fused glass by shock-wave compression, *Phys. Chem. Miner.*, *31*(8), 532–542, doi:10.1007/s00269-004-0408-9.

Tschauner, O., P. D. Asimow, N. Kostandova, T. J. Ahrens, C. Ma, S. Sinogeikin, Z. Liu, S. Fakra, and N. Tamura (2009), Ultrafast growth of wadsleyite in shock-produced melts and its implications for early solar system impact processes, *Proc. Natl. Acad. Sci. U. S. A.*, *106*(33), 13,691–13,695, doi:10.1073/pnas.0905751106.

Xue, X., and M. Kanzaki (2008), Structure of hydrous aluminosilicate glasses along the diopside-anorthite join: A comprehensive one- and two-dimensional ^{1}H and ^{27}Al NMR study, *Geochim. Cosmochim. Acta*, *72*(9), 2331–2348, doi:10.1016/j.gca.2008.01.022.

Xue, X., J. F. Stebbins, M. Kanzaki, P. F. McMillan, and B. Poe (1991), Pressure-induced silicon coordination and tetrahedral structural changes in alkali silicate melts up to 12 GPa: NMR, Raman, and infrared spectroscopy, *Am. Mineral.*, *76*(1–2), 8–26.

Yarger, J. L., K. H. Smith, R. A. Nieman, J. Diefenbacher, G. H. Wolf, B. T. Poe, and P. F. McMillan (1995), Al coordination changes in high-pressure aluminosilicate liquids, *Science*, *270*, 1964–1967, doi:10.1126/science.270.5244.1964.

P. Asimow, Division of Geological and Planetary Sciences, California Institute of Technology, 1200 E. California Blvd., Mail Code 170-25, Pasadena, CA 91125, USA.

L. Bai and O. Tschauner, High Pressure Science and Engineering Center, Department of Geology/Physics and Astronomy, University of Nevada, Las Vegas, 4505 S. Maryland Pkwy., Las Vegas, NV 89154-4002, USA.

P. Chow and Y. Xiao, HPCAT, Geophysical Laboratory, Carnegie Institution of Washington, 9700 South Cass Ave., Argonne, IL 60439, USA.

H.-I. Kim, S. K. Lee, and S. Y. Park, School of Earth and Environmental Sciences, Seoul National University, Seoul 151-742, South Korea. (sungklee@snu.ac.kr)